JPET Fast Forward. Published on February 26, 2013 as DOI: 10.1124/jpet.112.200808
This article has not been copyedited and formatted. The final version may differ from this version.

Title Page

The heme oxygenase system selectively enhances the anti-inflammatory macrophage-M2 phenotype, reduces pericardial adiposity and ameliorated cardiac injury in diabetic cardiomyopathy in Zucker diabetic fatty rats

Ashok Jadhav[†], Shuchita Tiwari[†], Paul Lee and Joseph Fomusi Ndisang

AJ, ST, PL and JFN: Department of Physiology, University of Saskatchewan College of Medicine

JPET Fast Forward. Published on February 26, 2013 as DOI: 10.1124/jpet.112.200808
This article has not been copyedited and formatted. The final version may differ from this version.

Running Title Page

Running title: Hemin abates pericardial adiposity

Corresponding author:
Dr. Joseph Fomusi Ndisang,
Department of Physiology,
College of Medicine,
University of Saskatchewan
107 Wiggins Road,
Saskatoon, SK,
Canada S7N 5E5.
Tel: (306) 966-6533
Fax: (306) 966-4298
E-mail: joseph.ndisang@usask.ca

Total number of text pages (including references and figure legends): 27
Total word count manuscript: 5257
Number of figures: 6
Number of tables: 2
Number of References: 57

Word count Abstract: 250
Introduction: 465
Discussion: 1438

Abbreviations
Activating protein 1 (AP-1)
Blood pressure (BP)
c-Jun-N-terminal kinase (cJNK),
Endothelin (ET-1)
End diastolic volume (EDV)
Enzyme Immunoassay (EIA)
Enzyme-linked immunosorbent assay (ELISA)
Heme oxygenase (HO)
Insulin receptor substrate 1 (IRS-1)
Interleukin (IL)
Left-ventricular systolic pressure (LVSP)
Nuclear factor kappaB (NF-κB)
Phosphatidylinositol-3-kinase (PI3K)
Protein kinase B (PKB)
Quantitative real time polymerase chain reaction (qRT-PCR)

Stannous mesoporphyrin (SnMP)
Tumour necrosis factor alpha (TNF-α)
Zucker diabetic fatty rats (ZDF)
Zucker Lean rats (ZL)

Abstract

Cardiac function is adversely affected by pericardial adiposity. We investigated the effects of the hemeoxygenase (HO) inducer, hemin on pericardial adiposity, macrophage polarization and diabetic cardiopathy in Zucker diabetic fatty rats (ZDFs) using echocardiographic, qRT-PCR, Western immunoblotting, EIA and spectrophotometric analysis. In ZDFs, hemin administration increased HO activity, normalised glycemia, potentiated insulin signalling by enhancing IRS-1, PI3K and PKB/Akt, suppressed pericardial adiposity, cardiac hypertrophy and left-ventricular longitudinal muscle fiber thickness, a pathophysiological feature of cardiomyocyte hypertrophy and correspondingly reduced systolic blood pressure, total peripheral resistance, pro-inflammatory/oxidative mediators including NF-κB, cJNK, ET-1, TNF-α, IL-6, IL-1β, AP-1 and 8-isoprostane, whereas the HO inhibitor, stannous mesoporphyrin (SnMP) nullified the effects. Furthermore, hemin reduced the pro-inflammatory macrophage M1 phenotype, but enhanced the M2 phenotype that dampens inflammation. Since NF-κB activates TNFα, IL6 and IL-1β, while TNF-α, JNK and AP-1 impair insulin signalling, the high levels of these cytokines in obesity/diabetes would create a vicious cycle that together with 8-isoprostane and ET-1 exacerbates cardiac injury, compromising cardiac function. Therefore, the concomitant reduction of pro-inflammatory cytokines and macrophage infiltration coupled to increased expressions of IRS-1, PI3K, PKB may account for enhanced glucose metabolism and amelioration of cardiac injury and function in diabetic cardiomyopathy. The hemin-induced preferential polarization of macrophages towards anti-inflammatory macrophage M2 phenotype in cardiac tissue with concomitant suppression of pericardial adiposity in ZDFs are novel findings. These data unveil the benefits of hemin against pericardial adiposity, impaired insulin signalling and diabetic cardiomyopathy, and suggest that its multifaceted protective mechanisms include the suppression of inflammatory/oxidative mediators.

INTRODUCTION

The inflammatory and metabolic systems have been evolutionarily well-conserved in species, and are fundamental for survival (Hotamisligil, 2006). However, these systems can be offset by obesity or nutrition-overload leading to inflammation in metabolic sites like the adipose tissue and skeletal muscles. Generally, obesity and insulin resistance are closely associated with a state of low-grade inflammation due to incessant activation of a wide variety of inflammatory mediators including nuclear factor kappaB (NF-κB), tumour necrosis factor-alpha (TNF-α) and cJun-N-terminal kinase (JNK) (Feinstein et al., 1993; Hotamisligil et al., 1993; Hotamisligil and Spiegelman, 1994; Uysal et al., 1997; Permana et al., 2006; Tuncman et al., 2006; Sabio et al., 2008; Tilg and Moschen, 2008; Fernandez-Veledo et al., 2009; Karalis et al., 2009; Scazzocchio et al., 2009; Ndisang, 2010). Moreover, NF-κB stimulates TNF-α, interleukin (IL)-6 and IL-1β, which in turn may activate JNK to create a vicious cycle that may aggravate insulin resistance and tissue damage (Ndisang, 2010). These destructive processes may be further exacerbated by macrophage infiltration, an event characterized by elevated levels of ED-1 (ED-1 is the primary antibody for activated macrophage (Bazan et al., 2012). Generally, macrophages express distinct patterns of surface receptors when responding to different stimuli. Currently, two distinct polarization states of macrophages, “classical” or M1 and “alternative” or M2 have been characterized (Gordon and Martinez, 2010; Ndisang, 2010). While the M1 phenotype promotes inflammation, the M2 phenotype dampens inflammatory events. Therefore, the concomitant reduction of M1 phenotype, NF-κB, TNF-α, JNK, IL6 and IL-1β would limit tissue insults and decrease the oxidative destruction of important metabolic regulators like adiponectin and insulin in type-2 diabetes (T2D) (Kamigaki et al., 2006; Kaneto et al., 2006).

Emerging evidence indicate that adipocytes from different body compartments have distinct inflammatory phenotype based on their anatomical location (Hamdy et al., 2006). Generally,

JPET Fast Forward. Published on February 26, 2013 as DOI: 10.1124/jpet.112.200808
This article has not been copyedited and formatted. The final version may differ from this version.

pericardial or ectopic adiposity is more-malignant than subcutaneous adiposity, although they are both implicated in the pathogenesis of obesity-related cardio-metabolic complications like insulin resistant T2D and coronary artery disease in lean and obese individuals (Hamdy et al., 2006; Rosito et al., 2008). Although we recently reported the insulin sensitizing effects of the heme oxygenase (HO) inducer, hemin, in Zucker diabetic Fatty rats (ZDF) (Ndisang et al., 2009), the effects of the HO system on pericardial adiposity remains largely unclear. Similarly, the effect of upregulating the HO system with hemin on macrophage polarization in cardiac tissue has not been reported. Whether hemin therapy will improve cardiac function in ZDF after suppressing M1 phenotype, NF-κB, TNF-α, JNK, IL6 and IL-1β in the left ventricle will be investigated. Therefore this study was designed to investigate the role of hemin on pericardial adiposity and the mechanisms by which hemin ameliorates diabetic cardiopathy in ZDF, an insulin-resistant T2D model with diabetic cardiomyopathy (Poornima et al., 2006; van den Brom et al., 2010).

MATERIALS AND METHODS (Extended methodology is available on supplemental file)

Animal treatment and biochemical assays

Our experimental protocol was approved by the University of Saskatchewan Standing Committee on Animal Care and Research Ethics, which is in conformity with the Guide for Care and Use of Laboratory Animals stipulated by the Canadian Council on Animal Care and the National Institutes of Health (NIH Publication No. 85-23, revised 1996). Twelve-week-old male ZDF rats, a genetically obese leptin receptor-deficient (*fa/fa*) animal model of T2D and their corresponding age/sex-matched Zucker-lean (ZL) littermates were purchased from Charles River (Willington, MA, USA). The animals were housed at 21°C with 12-hour light/dark cycles, fed with standard laboratory chow and had access to drinking water *ad libitum*. The drugs used for this study hemin, an inducer of HO (30 mg/kg i.p., Sigma, St Louis, MO) and stannous-mesoporphyrin

JPET Fast Forward. Published on February 26, 2013 as DOI: 10.1124/jpet.112.200808
This article has not been copyedited and formatted. The final version may differ from this version.

(SnMP), a blocker of HO (2 mg/100 g body weight ip, Porphyrin Products, Logan, UT). The doses of SnMP and hemin used in this study have been shown to be effective in previous studies (Goodman et al., 2006; Li et al., 2008; Ndisang and Jadhav, 2009a; Ndisang et al., 2009; Ndisang et al., 2010). Hemin and SnMP were prepared as we previously reported and were given biweekly for eight weeks (Goodman et al., 2006; Jadhav et al., 2008; Li et al., 2008; Ndisang and Jadhav, 2009a; Ndisang et al., 2009; Ndisang et al., 2010). Hemin has been approved by the FDA against porphyria (Anderson and Collins, 2006), while SnMP has successfully completed phase-III clinical trials (Anderson et al., 2005). At 14 weeks of age, the animals were randomly assigned to five experimental groups (*n=6-14* per group): **(A)** controls (ZDF and ZL), **(B)** hemin-treated ZDF and ZL, **(C)** ZDF+hemin+SnMP, **(D)** ZDF+SnMP and (**E**) ZDF+vehicle dissolving hemin and SnMP.

During the treatment period glucose was monitored weekly after 6 hrs of fasting in metabolic cages with a glucose-meter (BD, Franklin Lakes, NJ, USA). Body weight was also measured on a weekly basis. At the end of the 8-week treatment period, the animals were 22 weeks of age. A day prior to sacrifice, the animals were fasted in metabolic cages for 24-hr urined collection and weighed. Systolic blood pressure was determined by non-invasive tail-cuff method (Model 29-SSP, Harvard Apparatus, Montreal, Canada). Plasma was collected by intra-cardiac puncture and the pericardial fat pad and the heart were isolated, cleaned and weighed using an analytical balance (Precisa Instruments Ltd, Switzerland). The atria were removed from the heart and the right ventricle free wall separated from the left ventricle including the septum as we previously reported (Jadhav et al., 2008).

Left-ventricular HO activity was evaluated spectrophotometrically as bilirubin production using our established method (Jadhav et al., 2008; Ndisang et al., 2009; Ndisang and Jadhav, 2010;

JPET Fast Forward. Published on February 26, 2013 as DOI: 10.1124/jpet.112.200808
This article has not been copyedited and formatted. The final version may differ from this version.

Ndisang et al., 2010), while HO-1 (Stressgen-Assay Design, Ann Arbor, MI, USA), TNF-α, IL-6, IL1-β (Immuno-Biological Laboratories Co Ltd, Takasaki-shi, Gunma, Japan) were measured by commercially available ELISA kits. Other biochemical parameters such as left-ventricular 8-isoprostane and endothelin-1 were measured by EIA (Cayman Chemical, Ann Arbor, MI) as we previously reported (Jadhav et al., 2008; Ndisang and Jadhav, 2010).

Measurement of cardiac hemodynamic parameters (invasive hemodynamic measurements)

The animals were anesthetized with isoflurane through inhalation using vaporizer. The vaporizer was set at 5.0% isoflurane/L O_2(g) to induce, and 2.0%/L O_2(g) for maintenance of anesthesia. To measure the hemodynamic parameters, a Millar Mikro-Tip ultra-miniature tip sensor pressure transducer catheter (SPR-407) with a catheter size of 1.5 French was inserted through the right carotid artery and advanced into the left ventricular chamber to measure the left ventricular hemodynamic parameters. After positioning of the pressure transducer into the left ventricle, the rat was allowed to stabilize for 10 minutes before the left ventricular hemodynamic measurements were recorded. Arterial blood pressure was subsequently recorded by pulling the catheter out of the ventricular chamber into the aorta. Central venous pressure was measured by inserting the miniature tip sensor pressure transducer catheter into the superior vena cava through the right jugular vein. Data was acquired on a Biopac Data Acquisition system and assessed on AcqKnowledge software as previously reported (Jadhav et al., 2008; Senanayake et al.).

Echocardiography

Echocardiographic evaluation was done in rats using a Vevo 660 high frequency ultrasound machine (VisualSonics, Markham, ON) equipped with B-mode imaging. For consistency, all measurements were done by the same investigator and all ultrasound procedures did not exceed 30

minutes for each rat. Prior to ultrasound experiments, anaesthesia was induced with 5% isoflurane, maintained at 0.5-1% isoflurane (Abbott Laboratories, Saint-Laurent, QC), and the rats placed with the ventral side up on an electrocardiogram (ECG) plate (VisualSonics, Markham, ON) with each paw covered with electrode cream (Signa Crème, Parker Laboratories, Fairfield, NJ) and secured to ECG contacts with surgical tape in order to monitor heart rate throughout each experiment. A temperature probe was inserted rectally to maintain internal body temperature at 37°C. To prevent artifact with this high resolution ultrasound system, the animal was depilated by wiping from the chest area with depilatory cream (Nair, New York, NY). Thereafter, EcoGel 200 (Eco-Med Pharmaceuticals, ON) was then applied to the thorax for ultrasound.

A RMV 710B scanhead was used to gather all parasternal short and long-axis views of the rat ventricle in B-mode. The areas of three different short axis views along the ventricle were measured and designated as A_1, A_2, A_3 while the ventricular length of one long axis view was measured and divided by four to give ventricular height (h). Using different short axis views at different levels of the ventricle compensates for irregularities in ventricular shape and greatly increases accuracy of chamber volume measurements (Ram et al., 2011). All of these values were measured at both systole and diastole using VisualSonics software (Markham, ON). With these values, end systolic and diastolic volumes in units of cm^3 (equivalent to ml) were each calculated for the left ventricle using: (Equation I) $V = (A_1+A_2)h +((A_3h)/2) + (\pi/6(h^3))$.

End systolic volume was subtracted from end diastolic volume to give stroke volume (V_S) in millilitres. Heart rate in beats per minutes for each rat was recorded at three different times throughout one imaging period and then averaged. Cardiac output (CO) in millilitres/minute was then determined using heart rate (f_H) and stroke volume (V_S): (Equation II) $CO = f_H * V_S$. Ejection fraction (%) for each rat was also calculated using stroke volume (V_S) and end diastolic volume (EDV): (Equation III) $E_f = V_S /EDV$

JPET Fast Forward. Published on February 26, 2013 as DOI: 10.1124/jpet.112.200808
This article has not been copyedited and formatted. The final version may differ from this version.

In order to measure left ventricular free wall thickness, a clip in parasternal long axis view was obtained for all experimental groups. At least three individual images were exported from the clip at both systole and diastole using Premiere Elements 2.0 (Adobe, San Jose, CA) and then left ventricular wall thickness determined using ImagePro 6.0 software (Bethesda, MD). Heart rate (f_H in beats per minute) was calculated from ECG traces during the blood pressure experiment.

Total RNA Isolation and Quantitative RT-PCR for p65-NF-κB, AP-1 and JNK

The left ventricle was homogenized and quantitative RT-PCR done as we previously reported (Jadhav et al., 2008; Ndisang et al., 2009; Ndisang et al., 2010). Briefly, triplicate samples of 1 µl of cDNA each was ran using a template of 3.2 pmol of primers for NF-κB (forward, 5'CATGCGTTTCCGTTACAAGTGCGA-3' and reverse 5'TGGGTGCGTCTTAGTGGTATCTGT-3'), AP-1 (forward, 5'AGCAGATGCTTGAGTTGAGAGCCA3' and reverse, 5'TTCCATGGGTCC CTGCTTTGAGAT-3'), JNK (forward 5′AAGCAGCAAGGCTACTCCTTCTCA-3′ and reverse 5′ATCGAGACTGCTGTCTGTGTCTGA-3′) and glyceraldehyde-3-phosphate dehydrogenase (GAPDH) (forward 5′AGCAAGGATACTGAGAGCAAGA-3' and reverse 5'TCTGGGATGGAA TTGTGAGGGAGA-3') in a final volume of 25 µl. Sequences of all primers were confirmed by the National Research Council of Canada, Saskatoon.

Western Immunoblotting

The left ventricular tissue was homogenized and centrifuged as previously described (Jadhav et al., 2008; Ndisang et al., 2008; Ndisang et al., 2009; Ndisang et al., 2010). Primary antibodies (Santa Crutz Biotechology, CA, USA) including ED-2 (sc-58956), ED-1 (sc-59103), phosphatidylinositol-3-kinase (PI3K) (sc67306), protein kinase-B (PKB) (sc9118) and insulin-receptor-substrate-1 (IRS-1) (8299) were used. Densitometric analysis was done with UN-SCAN-IT

software (Silk Scientific, Utah, USA). GAPDH antibody (Sigma St Louis, MO, USA) was used as a control to ascertain equivalent loading.

Left Ventricular Histology

The middle portion (midpapillary level) of the left ventricle of heart was separated, fixed in 10 % formalin phosphate buffer for 48 hrs, processed and paraffin embedded as we previously reported (Jadhav et al., 2008). Then sections of 5 μm thicknesses were cut and stained with hematoxylin and eosin for histological analysis. The left ventricular sections were obtained from the middle portion of the left ventricle to avoid differences in regional cardiomyocyte size in different regions of the left ventricle. The cardiac sections were scanned using a microscope (Aperio Scan Scope Model CS, Aperio Technology Inc, CA, USA) and analyzed using Aperio Image Scope V11.2.0.780 software (Aperio, e-Pathology Solution, CA USA). Left ventricular myocyte width longitudinal myocyte thickness was measured randomly in 20-30 cardiac muscle fibers from each left ventricular tissue section. Muscle fiber thickness was quantified and analyzed between different groups. For consistency, myocytes were positioned perpendicularly to the plane of the section with a visible nucleus and cell membrane clearly outlined. Unbroken areas were selected for measurement. All sections were imaged at 40X zoom (40X; 0.50 μm/pixel) in Apero Image Scope using length measurement tool (μmeter).

Statistical Analyses

All data were expressed as means ± SEM from at least six independent experiments unless otherwise stated. Statistical analyses were done using unpaired Student's *t*-test and analyses of

variance in conjunction with Bonferroni test for repeated measures where appropriate. Group differences at the level of $p<0.05$ were considered statistically significant.

RESULTS

Hemin therapy abated pericardial adiposity and restored normoglycemia in ZDF rats

ZDF rats were severely hyperglycemic with fasting glucose levels of 24.6 ± 3.1 mmol/L (**Table-1**), whereas their age/sex matched littermates control-ZL were normoglycemic (7.2 ± 0.8 mmol/L). The 8-week regimen of hemin to ZDF reduced the elevated glycemia to physiological level (24.6 ± 3.1 vs. 6.8 ± 1.3 mmol/L; $p<0.01$), whereas the co-treatment of hemin and the HO inhibitor, SnMP abolished the effect of hemin, suggesting a role of the HO system on glucose homeostasis. Similarly, hemin treatment significantly reduced pericardial adiposity (1.85 ± 0.2 vs. 0.79 ± 0.13 g/Kg body weight, $p <0.01$) and cardiac hypertrophy (3.8 ± 0.3 vs. 2.4 ± 0.14 g/Kg body weight; $p<0.01$) in ZDF, whereas the co-administration of hemin and SnMP nullified the effect, suggesting a role of the HO system on the regulation of pericardial adiposity and cardiac hypertrophy. The vehicle dissolving hemin and SnMP had no effect on blood glycemia, pericardial adiposity and heart weight (**Table-1**).

Hemin therapy also affected ZL rats though less intensely. A slight but significant reduction of blood glucose, cardiac hypertrophy and pericardial adiposity was observed ZL rats. These effects were abolished by SnMP (**Table-1**). In hemin-treated ZDF rats, blood glucose, cardiac hypertrophy and pericardial adiposity were reduced by 72.3, 36.8 and 57% respectively whereas in ZL rats these same parameters were reduced by 11.1, 14.8 and 25.4% respectively, suggesting greater selectivity of the actions of hemin in diseased conditions like the situation in ZDF rats, whereas less active in healthy status as in the case of ZL rats.

The HO inducer, hemin and HO blocker, SnMP also affected body weight. A slight body-weight loss (< 10%) was observed in hemin- and SnMP-treated animals (**Table 1**). In ZL+hemin, ZDF+hemin, and ZDF+hemin+SnMP the loss of body weight were 2.5, 5.3 and 8.1% respectively. Although body-weight loss can affect blood glucose levels, it is unlikely in this case since the slight body-weight loss in hemin- and SnMP-treated were accompanied by opposite effects on glucose levels (**Table 1**). Accordingly, we observed a decrease of glucose levels in hemin-treated animals, but an increase in SnMP-treated animals suggesting that the HO system may be endowed with intrinsic anti-diabetic effects. The loss of body weight may not be due to toxicity as we recently showed that several indices of toxicity including plasma gamma-glutamyltransferase (γGGT), aspartate aminotransferase (AST) and alanine aminotransferase (ALT) were within normal range (Ndisang et al., 2009).

Hemin therapy also improved cardiac hemodynamics (**Table-2)**. In hemin-treated ZDF, systolic blood pressure was reduced by 13.95%, while cardiac output increased by 8.2%. Interestingly, the lowering of systolic blood pressure was associated with a 12.2% decrease in total peripheral resistance, suggesting reduced afterload to the left ventricle (Boron and Boulpaep, 2009). Correspondingly, a reduction of 8.9% in the rate of left-ventricular pressure development (+dP/dt) was observed (**Table-2)**. Furthermore, hemin increased the left-ventricular ejection fraction by 5.4%, and this effect was accompanied by a 2.2 % reduction of left-ventricular systolic pressure (LVSP). Therefore, increased cardiac output coupled to the concomitant reduction of total peripheral resistance, +dP/dt and LVSP are indicative of improved cardiac function in hemin-treated ZDF.

Hemin therapy enhanced HO-1 and HO activity but abated ET-1 and 8-isoprostane in the left ventricle of ZDF rats

To investigate the role of the HO system in the improved cardiac function and insulin-signalling in ZDF, we measured HO activity, ET-1 and 8-isoprostane. Our results indicate that the basal levels of HO-1 and HO activity in control-ZDF were significantly reduced by 2.13- and 1.98-fold respectively as compared to control-ZL rats. Hemin therapy markedly increased the depressed levels of HO-1 and HO activity in ZDF rats by 8.1- and 10.56-fold respectively (**Figs. 1A and 1B)**, whereas the co-treatment with the HO inhibitor, SnMP nullified the effects of the HO inducer, hemin. Similarly, treatment with SnMP alone depleted the basal levels of HO-1 and HO activity (**Figs. 1A and 1B**). Hemin therapy also enhanced the levels of HO-1 and HO activity in ZL rats, although a greater increment was observed in hemin-treated ZDF animals (**Figs. 1A and 1B**). The higher magnitude of HO signalling may be responsible for the more intense reduction of glycemic levels in ZDF rats as compared to ZL rats (**Table-1**). Alternatively, the less preponderant increase of HO activity in ZL rats may suggest greater stability of the HO system in healthy conditions.

Given that elevated oxidative stress is among the causative factors of insulin resistance and cardiac dysfunction, we measured 8-isoprostane, an important marker of oxidative stress (Delanty et al., 1997). In ZDF rats, the basal levels of left-ventricular 8-isoprostane were markedly elevated, suggesting enhanced oxidative stress (**Fig. 1C**). Interestingly, hemin therapy significantly reduced 8-isoproatane by 57.6%. Contrarily, in SnMP+ZDF-treated animals, the effect of hemin on 8-isoprostane was annulled and 8-isoprostane was reversed to comparable levels as observed in control-ZDF rats. On the other hand, in SnMP-treated animals, the levels of left-ventricular 8-isoprostane were further increased, suggesting that oxidative stress is further potentiated by blockade of basal HO activity (**Fig. 1C**). Hemin therapy also reduced 8-isoprostane in ZL rats,

although less intensely as compared to ZDF as only a 28.9% reduction was observed in hemin-treated ZL rats as compared to 57.6% hemin-treated ZDF rats.

Since 8-isoprostane stimulates ET-1 (Fukunaga et al., 1995), and both ET-1 and 8-isoprostane are involved in the oxidative destruction of tissue, we also assessed ET-1 in the left ventricle. Our results indicate that the levels of ET-1 in ZDF rats were 2.7-fold higher than in control-ZL rats. Interestingly, hemin therapy greatly attenuated the elevated levels of left-ventricular ET-1 in ZDF rats, while SnMP abolished the effect of hemin (**Fig. 1D**). Hemin therapy also reduced ET-1 levels in ZL rats albeit to a lesser extent as compared to ZDF rats. Accordingly, a reduction of 25.2% of ET-1 was observed in hemin-treated ZL rats as compared to 54.2% hemin-treated ZDF rats.

Therefore, the preponderant increase of HO activity in hemin-treated ZDF as compared to hemin-treated ZL (**Figs. 1A**), coupled to the more accentuated reduction of left-ventricular 8-isoprostane (**Fig. 1C**) and ET-1 (**Fig. 1D)** may account for the greater anti-diabetic effect (**Table-1**) and improved cardiac effects (**Table-2**) in hemin-treated ZDF.

Hemin therapy suppressed pro-inflammatory cytokines that deregulate glucose metabolism cardiac function

TNF-α, IL-6 and IL-1β are cytokines that impair cardiac function and glucose metabolism (Li et al., 2006; Burgess et al., 2010; Ndisang, 2010), so we investigated whether the improvement in cardiac function and glucose metabolism in hemin-treated ZDF would be accompanied by reduction of these cytokines. Our results indicate that the levels of TNF-α, IL-6 and IL-1β in the left ventricle of control-ZDF rats were significantly elevated by 4.5-, 9.1- and 2.5-fold respectively as compared to control-ZL rats (**Fig. 2**). Treatment with hemin markedly reduced TNF-α, IL-6 and IL-

1β by 71.2, 51.3 and 56.8% respectively. In contrast, the co-application of the HO inhibitor, SnMP with hemin reversed the effects of hemin (**Figs. 2A, 2B and 2C**), suggesting a role of the HO system in the regulation of these inflammatory cytokines. Hemin therapy also reduced the levels of TNF-α, IL-6 and IL-1β in the ZL rats, although less intensely. A reduction of 35.4, 37.0, 28.5% of TNF-α, IL-6 and IL-1β respectively was observed in hemin-treated ZL rats as compared to 71.2, 51.3, 56.8% in hemin-treated ZDF rats.

Hemin abated transcription factors that impair insulin-signalling and cardiac function

Many inflammatory and oxidative transcriptions factors including NF-κB, AP-1 and JNK are implicated in tissue damage and insulin resistance (Bennett et al., 2003; Kaneto et al., 2006). In ZDF rats, quantitative real-time RT-PCR analyses indicated that the levels of NF-κB, AP-1 and JNK in the left ventricle were strikingly elevated (**Fig. 3**). Treatment with hemin reduced NF-κB and AP-1 by 2.5- and 2.9-fold respectively, while the HO inhibitor, SnMP, nullified the effects of hemin (**Fig. 3A and 3B**). Moreover, treatment with SnMP alone further enhanced NF-κB and AP-1 in ZDF rats by 20% and 31.9% respectively, suggesting the involvement of basal HO activity in the regulation of these oxidative/inflammatory mediators. Furthermore, in ZDF rats, the basal expression of left-ventricular JNK, a substance that suppresses insulin biosynthesis (Kaneto et al., 2006), was markedly increased by 4.75-fold, but was abated by hemin (**Fig. 3C**). Hemin therapy also reduced NF-κB, AP-1 and JNK in ZL rats by 30.5, 24.8, and 26.1% respectively which were less intense as compared to hemin-treated ZDF where the reduction of NF-κB, AP-1 and JNK were 59.3, 65.6 and 57.8%, suggesting greater selectivity of hemin in diseased condition.

Hemin therapy abated inflammation but potentiated insulin-signalling agents

Given that macrophages are amongst the fundamental sources of many of the circulating inflammatory molecules in obesity, and are postulated to be causal in the development of insulin-resistant T2D (Gordon and Martinez, 2010; Ndisang, 2010), we used specific markers (ED1 and ED2) to quantify the M1 pro-inflammatory phenotype (ED1) and the M2 anti-inflammatory phenotype (ED2). Our Western immunoblotting and relative densitometric analyses indicated that the expression of the pro-inflammatory M1 phenotype in control-ZDF was significantly elevated (**Fig. 4A**), but interestingly was abated by 40.1% by hemin therapy. On the other hand, the anti-inflammatory phenotype, M2, was significantly reduced in control-ZDF (**Fig. 4B**), but interestingly was enhanced by 61.3% by hemin therapy, suggesting that hemin may preferentially favour macrophage polarization towards the M2 anti-inflammatory phenotype as an alternative mechanism to counteract tissue insult.

Given that IRS1, PI3K and PKB are important proteins implicated in the insulin signal transduction pathway (Ndisang, 2010), we investigated the effect of hemin therapy on these proteins. Our results indicate that the expression of IRS1 in control-ZDF was depressed (**Fig. 4C**). However, hemin therapy greatly enhanced the expression of IRS1 bv 2.3-fold. Similarly hemin therapy significantly increased the expressions of PI3K (**Fig. 4D**) and PKB (**Fig. 4E**) by 3.5-and 2.8-fold respectively.

Hemin therapy reduced longitudinal muscle fiber thickness in ZDF rat

Longitudinal muscle fiber thickness is common pathophysiological feature of cardiac myocyte hypertrophy (Conrad et al., 1995; Rodriguez et al., 2005; Jadhav et al., 2008). In untreated ZDF rats, enlarged cardiomyocytes with increscent nuclei were evident, as compared to normal cardiomyocytes in ZL-control rats (**Fig. 5A**). The inter myofibril space was reduced in ZDF-control

rats as compared to the age/sex-matched ZL rats (**Fig. 5A**). Indeed, a 44 % increase in cardiomyocyte longitudinal fiber thickness was observed in the ZDF-control rats as compared to ZL rats (21.9 ± 0.89 vs 15.2 ± 0.49 μmetre, $p<0.01$, n=6) (**Fig. 5B**). Interestingly, hemin treatment reduced cardiomyocyte longitudinal fiber thickness by 25 % as compared to ZDF control (18.1 ± 0.76 vs 21.9 ± 0.89 μmetre, $p<0.05$, n=6). However, this reduction did not reach the basal level of cardiomyocyte longitudinal thickness of the ZL rats (15.2 ± 0.49 μmetre) (**Fig. 5B**).

DISCUSSION

The present study demonstrates for the first time that upregulating the HO system with hemin preferentially favors macrophage polarization towards the M2 phenotype that dampens inflammation, while suppressing the M1 pro-inflammatory phenotype. Another novel observation is that hemin therapy suppresses pericardial adiposity in ZDF rats, a model of insulin resistance, dyslipidemia, hyperglycaemia and diabetic cardiomyopahy (Poornima et al., 2006; Ndisang et al., 2009; van den Brom et al., 2010). Pericardial adiposity and cardiac hypertrophy are associated with elevated inflammatory/oxidative insults and dyslipidemia that adversely affect cardiac function, especially in individuals co-morbid with obesity and insulin resistance (Hamdy et al., 2006; Jadhav et al., 2008; Rosito et al., 2008; McAuley et al., 2011). Interestingly, hemin therapy significantly reduced pericardial adiposity and cardiac hypertrophy, and attenuated macrophage infiltration and several pro-inflammatory/oxidative mediators, such as NF-κB, AP-1 JNK, TNF-α, IL-6 and IL-1β (Bennett et al., 2003; Kaneto et al., 2006; Li et al., 2006; Burgess et al., 2010; Ndisang, 2010),

but enhanced important proteins involved in the insulin signal transduction pathway such as IRS-1, PI3K, and PKB (Ndisang, 2010), with corresponding reduction of hyperglycemia in ZDF.

The hemin-dependent preferential enhancement of the M2-phenotype may be considered a novel and alternative anti-inflammatory mechanism through which the HO system counteracts inflammatory insult. Although one study had previously reported the role of HO-1 promoter in macrophage polarization (Weis et al., 2009), the expression levels of M1 and M2 phenotypes were not measured, so our study provides the first solid evidence on the role of the HO system on macrophage polarization. Besides macrophage infiltration, the HO system may reduce tissue inflammation through other mechanisms including the suppression of inflammatory cytokines like TNF-α, IL-6 and IL-1β (Li et al., 2006; Burgess et al., 2010; Ndisang, 2010). Consistently, in hemin-treated ZDF rats, TNF-α, IL-6 and IL-1β were markedly reduced. Similarly, other pro-inflammatory/oxidative mediators such as 8-isoprostane, NF-κB, AP-1 and JNK (Bennett et al., 2003; Kaneto et al., 2006) were greatly attenuated by hemin therapy, whereas the HO inhibitor, SnMP, nullified the hemin effects and exacerbated oxidative/inflammatory insults causing further impairment in glucose metabolism.

Another important observation from our study is the attenuation of cardiac hypertrophy and and the corresponding reduction of left-ventricular longitudinal muscle-fiber thickness, a common pathophysiological feature of cardiaomyocyte hypertrophy (Conrad et al., 1995; Rodriguez et al., 2005; Jadhav et al., 2008). Other mechanisms that may be responsible for the improvement of cardiac hemodynamic parameters by the HO system include vascular contractility (Sammut et al., 1998), ventricular contractility (Achouh et al., 2005), and the reduction of cardiac injury (Conrad et al., 1995; Rodriguez et al., 2005; Jadhav et al., 2008; Jadhav and Ndisang, 2009; Ndisang and Jadhav, 2009b), which would result in a healthier heart with improved ventricular contractility and

improved hemodynamics (Achouh et al., 2005). Furthermore, the HO system generates a vasodilator like carbon monoxide, a stimulator of cGMP that modulates both vascular contractility (Sammut et al., 1998; Achouh et al., 2005) and ventricular contractility thus hemodynamics (Achouh et al., 2005). Interestingly, in the present study the abrogation of cardiac hypertrophy and longitudinal muscle-fiber thickness were associated with also improved cardiac hemodynamics. In particular, systolic blood pressure was significantly lowered while cardiac output increased by 8.3% in hemin-treated ZDF. The lowering of systolic blood pressure and left-ventricular systolic pressure observed were accompanied by the reduction of total-peripheral resistance, and these effects would reduce the afterload to the left ventricle and thus prevents the onset of ventricular dysfunction (Awan et al., 1981; Boron and Boulpaep, 2009; Pingitore et al., 2011). An abnormal left ventricular function would affect the cardiac performance and contributes to the symptoms associated with cardiac failure (Heidenreich et al., 2012). With the reduction of systolic blood pressure in hemin-treated ZDF, left ventricular cardiomyocytes would contract less vigorously. This was evidenced by the reduction of +dP/dt. Therefore, by not generating a high pressure gradient to maintain adequate blood circulation, the workload and oxygen consumption by the left ventricle would be reduced and the risk of cardiovascular related morbidity and mortality would be curtailed (Awan et al., 1981; Boron and Boulpaep, 2009; Pingitore et al., 2011; Heidenreich et al., 2012).

Hemin therapy also enhanced the HO system and abated NF-κB, AP-1 JNK, TNF-α, IL-6 and IL-1β in ZL-control rats, although the magnitude was smaller as compared to ZDF rats with depressed HO activity. The reasons for this selective effect of HO are not fully understood. However, it is possible that since ZL rats are healthy animals with normal/functional insulin signalling, the HO system may be more stable as compared to ZDF which have depressed HO activity. Importantly, the selectivity of the HO system in diseased conditions could be explored against the co-morbidity of insulin resistant diabetes and obesity. Nevertheless, future studies will

be done to investigate the selective effects of the HO system on ZL-control rats. Although we previously reported the insulin sensitizing effect of hemin in the gastrocnemius muscle of ZDF, tissue-specific response is a well-known phenomenon in the pathophysiology of insulin resistance and impaired glucose metabolism, and different tissues may respond distinctly to the same stimuli, indicating that a physiological response in one tissue may not necessarily be the same in another tissue (Farret et al., 2006; Zhang et al., 2010). Whether the reported effects were unique for the gastrocnemius muscle or universal for other tissues is critical for understanding the role of hemin in insulin resistance and glucose metabolism. Therefore, studying the effect of an upregulated HO system in the left ventricle of ZDF rat is important for the advancement of knowledge in this area. Moreover, the effects of hemin therapy on left-ventricular IRS-1, PI3K and PKB in ZDF-rat, a model with diabetic cardiomyopathy (Poornima et al., 2006; van den Brom et al., 2010) remains poorly understood. Interesting, the present study unveils that the restoration of normoglycemia in hemin-treated ZDF was accompanied by the concomitant potentiation of left-ventricular IRS-1, PI3K and PKB, and the improvement of cardiac hemodynamics, particularly the reduction of total-peripheral resistance and systolic blood pressure.

Collectively, our study unveils the beneficial effect of the HO system on pericardial adiposity, impaired insulin signalling, diabetic cardiomyopathy and suggest that the suppression of cardiac hypertrophy, left-ventricular longitudinal muscle-fiber-thickness alongside the reduction of inflammatory/oxidative mediators are among the multifaceted mechanisms by which the HO system maintains homeostasis in physiological milieu. Given that NF-κB activates TNFα, IL6 and IL-1β (Ndisang, 2010), while TNF-α, JNK and AP-1 impair insulin signalling (Ndisang, 2010), the high levels of these cytokines and inflammatory/oxidative mediators in the chronic conditions of obesity and diabetes would create a vicious cycle that when added to the oxidative insults generated by 8-isoprostane and ET-1 (Yura et al., 1999) would exacerbate cardiac insult and compromise

cardiac function. Therefore, the concomitant reduction of cardiac hypertrophy, left-ventricular longitudinal muscle-fiber-thickness, pro-inflammatory cytokines and macrophage infiltration coupled to the potentiation of insulin signal transduction agents such as IRS-1, PI3K and PKB may account for enhanced glucose metabolism and improved cardiac hemodynamics in hemin-treated ZDF. Importantly, the novel findings of our study includes: **(i)** the preferential polarization of macrophages towards anti-inflammatory M2-phenotype in cardiac tissue as evidenced by increased expression levels of the M2-phenotye and the parallel reduction of the M1-proinflammatory phenotype; **(ii)** the suppression of pericardial adiposity; and **(iii)** the hemin-induced improvement of cardiac hemodynamic, particularly the reduction of total-peripheral resistance in ZDF rat, a model of obsessed insulin resistant type-2 diabetes with cardiomyopathy (Poornima et al., 2006; van den Brom et al., 2010).

With the escalation of obesity, diabetes and hypertension in industrialized and developing countries, the incidence of cardio-metabolic complications including diabetic cardiomyopathy and heart failure will increase. Cardio-metabolic complications are multifactorial diseases and a wide variety of different pathophysiological factors including inflammatory/oxidative insults are involved. The present study highlights the ability of hemin therapy to suppress inflammatory/oxidative mediators and improve insulin signalling in type-2 diabetes. Impaired insulin signalling is not only an important etiological factor in the pathogenesis of type-1 and type-2 diabetes, but also an important patho-physiological driving force that is capable of dictating the dynamics and progression of the disease as well as its ultimate evolution in to complications like diabetic cardiomyopathy. Therefore, the findings reported here could serve as a useful tool for the formulation of novel therapeutic agents against diabetes, pericardial adiposity and related complications like diabetic cardiomyopathy. Interestingly, our study may have great translational potential as the drugs used (hemin and SnMP) may have therapeutic application. Both hemin and

SnMP may have application in clinics as hemin has been approved by the FDA against porphyria (Buck, 1995; Anderson and Collins, 2006), while SnMP has successfully completed phase-III clinical trials for possible use against neonatal jaundice (Alexander, 2004; Kappas, 2004; Anderson, 2005).

ACKNOWLEDGEMENTS

The authors are grateful to James Talbot for technical assistance.

AUTHORSHIP CONTRIBUTION

Ashok Jadhav: Conducted experiments, performed data analysis and contributed to the writing of the manuscript.

Shuchita Tiwari: Conducted experiments, performed data analysis and contributed to the writing of the manuscript

Paul Lee: Conducted experiments and contributed to the writing of the manuscript

Joseph Fomusi Ndisang: Conceived the idea, designed the research, conducted experiments, performed data analysis and contributed to the writing of the manuscript.

REFERENCES

Achouh P, Simonet S, Badier-Commander C, Chardigny C, Vayssettes-Courchay C, Zegdi R, Khabbaz Z, Fabiani JN and Verbeuren TJ (2005) The induction of heme oxygenase 1 decreases contractility in human internal thoracic artery and radial artery grafts. *The Journal of thoracic and cardiovascular surgery* **130**:1573-1580.

Alexander D (2004) A method for interdicting the development of severe jaundice in newborns by inhibiting the production of bilirubin. *Pediatrics* **113**:135.

Anderson KE (2005) Studies in Porphyria III: Heme and Tin Mesoporphyrin in Acute Porphyrias (ClinicalTrials.gov Identifier NCT00004396), National Center for Research Resources (NCRR), 2005, http://www.clinicaltrials.gov/ct/show/NCT00004396

Anderson KE, Bloomer JR, Bonkovsky HL, Kushner JP, Pierach CA, Pimstone NR and Desnick RJ (2005) Recommendations for the diagnosis and treatment of the acute porphyrias. *Ann Intern Med* **142**:439-450.

Anderson KE and Collins S (2006) Open-label study of hemin for acute porphyria: clinical practice implications. *Am J Med* **119**:801 e819-824.

Awan NA, DeMaria AN, Miller RR, Amsterdam EA and Mason DT (1981) Beneficial effects of nitroprusside administration on left ventricular dysfunction and myocardial ischemia in severe aortic stenosis. *American heart journal* **101**:386-394.

Bazan NG, Eady TN, Khoutorova L, Atkins KD, Hong S, Lu Y, Zhang C, Jun B, Obenaus A, Fredman G, Zhu M, Winkler JW, Petasis NA, Serhan CN and Belayev L (2012) Novel aspirin-triggered neuroprotectin D1 attenuates cerebral ischemic injury after experimental stroke. *Exp Neurol* **236**:122-130.

Bennett BL, Satoh Y and Lewis AJ (2003) JNK: a new therapeutic target for diabetes. *Curr Opin Pharmacol* **3**:420-425.

Boron WF and Boulpaep E (2009) *Medical Physiology*. Saunders Elsevier, Philadelphia, MA.

Buck M (1995) Formulary update: Hemin injection (Panhematin) was approved for the treatment of intermittent porphyria. In Vancomycin: old controversies and new issues., in *Pediatric Pharmacotherapy*.

Burgess A, Li M, Vanella L, Kim DH, Rezzani R, Rodella L, Sodhi K, Canestraro M, Martasek P, Peterson SJ, Kappas A and Abraham NG (2010) Adipocyte heme oxygenase-1 induction attenuates metabolic syndrome in both male and female obese mice. *Hypertension* **56**:1124-1130.

Conrad CH, Brooks WW, Hayes JA, Sen S, Robinson KG and Bing OH (1995) Myocardial fibrosis and stiffness with hypertrophy and heart failure in the spontaneously hypertensive rat, in *Circulation* pp 161-170.

Delanty N, Reilly MP, Pratico D, Lawson JA, McCarthy JF, Wood AE, Ohnishi ST, Fitzgerald DJ and FitzGerald GA (1997) 8-epi PGF2 alpha generation during coronary reperfusion. A potential quantitative marker of oxidant stress in vivo. *Circulation* **95**:2492-2499.

Farret A, Filhol R, Linck N, Manteghetti M, Vignon J, Gross R and Petit P (2006) P2Y receptor mediated modulation of insulin release by a novel generation of 2-substituted-5'-O-(1-boranotriphosphate)-adenosine analogues. *Pharm Res* **23**:2665-2671.

Feinstein R, Kanety H, Papa MZ, Lunenfeld B and Karasik A (1993) Tumor necrosis factor-alpha suppresses insulin-induced tyrosine phosphorylation of insulin receptor and its substrates. *J Biol Chem* **268**:26055-26058.

Fernandez-Veledo S, Vila-Bedmar R, Nieto-Vazquez I and Lorenzo M (2009) c-Jun N-terminal kinase 1/2 activation by tumor necrosis factor-alpha induces insulin resistance in human

visceral but not subcutaneous adipocytes: reversal by liver X receptor agonists. *J Clin Endocrinol Metab* **94**:3583-3593.

Fukunaga M, Yura T and Badr KF (1995) Stimulatory effect of 8-Epi-PGF2 alpha, an F2-isoprostane, on endothelin-1 release. *J Cardiovasc Pharmacol* **26 Suppl 3**:S51-52.

Goodman AI, Chander PN, Rezzani R, Schwartzman ML, Regan RF, Rodella L, Turkseven S, Lianos EA, Dennery PA and Abraham NG (2006) Heme oxygenase-2 deficiency contributes to diabetes-mediated increase in superoxide anion and renal dysfunction. *J Am Soc Nephrol* **17**:1073-1081.

Gordon S and Martinez FO (2010) Alternative activation of macrophages: mechanism and functions. *Immunity* **32**:593-604.

Hamdy O, Porramatikul S and Al-Ozairi E (2006) Metabolic obesity: the paradox between visceral and subcutaneous fat. *Curr Diabetes Rev* **2**:367-373.

Heidenreich PA, Zhao X, Hernandez AF, Yancy CW and Fonarow GC (2012) Patient and hospital characteristics associated with traditional measures of inpatient quality of care for patients with heart failure. *American heart journal* **163**:239-245 e233.

Hotamisligil GS (2006) Inflammation and metabolic disorders. *Nature* **444**:860-867.

Hotamisligil GS, Shargill NS and Spiegelman BM (1993) Adipose expression of tumor necrosis factor-alpha: direct role in obesity-linked insulin resistance. *Science* **259**:87-91.

Hotamisligil GS and Spiegelman BM (1994) Tumor necrosis factor alpha: a key component of the obesity-diabetes link. *Diabetes* **43**:1271-1278.

Jadhav A and Ndisang JF (2009) Heme arginate suppresses cardiac lesions and hypertrophy in deoxycorticosterone acetate-salt hypertension. *Exp Biol Med (Maywood)* **234**:764-778.

Jadhav A, Torlakovic E and Ndisang JF (2008) Interaction Among Heme Oxygenase, Nuclear Factor-{kappa}B, and Transcription Activating Factors in Cardiac Hypertrophy in Hypertension. *Hypertension* **52**:910-917.

Kamigaki M, Sakaue S, Tsujino I, Ohira H, Ikeda D, Itoh N, Ishimaru S, Ohtsuka Y and Nishimura M (2006) Oxidative stress provokes atherogenic changes in adipokine gene expression in 3T3-L1 adipocytes. *Biochem Biophys Res Commun* **339**:624-632.

Kaneto H, Nakatani Y, Kawamori D, Miyatsuka T, Matsuoka TA, Matsuhisa M and Yamasaki Y (2006) Role of oxidative stress, endoplasmic reticulum stress, and c-Jun N-terminal kinase in pancreatic beta-cell dysfunction and insulin resistance. *Int J Biochem Cell Biol* **38**:782-793.

Kappas A (2004) A method for interdicting the development of severe jaundice in newborns by inhibiting the production of bilirubin. *Pediatrics* **113**:119-123.

Karalis KP, Giannogonas P, Kodela E, Koutmani Y, Zoumakis M and Teli T (2009) Mechanisms of obesity and related pathology: linking immune responses to metabolic stress. *Febs J* **276**:5747-5754.

Li M, Kim DH, Tsenovoy PL, Peterson SJ, Rezzani R, Rodella LF, Aronow WS, Ikehara S and Abraham NG (2008) Treatment of obese diabetic mice with a heme oxygenase inducer reduces visceral and subcutaneous adiposity, increases adiponectin levels, and improves insulin sensitivity and glucose tolerance. *Diabetes* **57**:1526-1535.

Li Y, Takemura G, Okada H, Miyata S, Maruyama R, Li L, Higuchi M, Minatoguchi S, Fujiwara T and Fujiwara H (2006) Reduction of inflammatory cytokine expression and oxidative damage by erythropoietin in chronic heart failure. *Cardiovasc Res* **71**:684-694.

McAuley PA, Hsu FC, Loman KK, Carr JJ, Budoff MJ, Szklo M, Sharrett AR and Ding J (2011) Liver attenuation, pericardial adipose tissue, obesity, and insulin resistance: the Multi-Ethnic Study of Atherosclerosis (MESA). *Obesity (Silver Spring)* **19**:1855-1860.

Ndisang JF (2010) Role of heme oxygenase in inflammation, insulin-signalling, diabetes and obesity. *Mediators Inflamm* **2010**:359732.

Ndisang JF and Jadhav A (2009a) Up-regulating the hemeoxygenase system enhances insulin sensitivity and improves glucose metabolism in insulin-resistant diabetes in Goto-Kakizaki rats. *Endocrinology* **150**:2627-2636.

Ndisang JF and Jadhav A (2009b) Upregulating the heme oxygenase system suppresses left ventricular hypertrophy in adult spontaneously hypertensive rats for 3 months. *J Card Fail* **15**:616-628.

Ndisang JF and Jadhav A (2010) Heme arginate therapy enhanced adiponectin and atrial natriuretic peptide, but abated endothelin-1 with attenuation of kidney histopathological lesions in mineralocorticoid-induced hypertension. *J Pharmacol Exp Ther* **334**:87-98.

Ndisang JF, Lane N and Jadhav A (2008) Crosstalk between the heme oxygenase system, aldosterone, and phospholipase C in hypertension. *J Hypertens* **26**:1188-1199.

Ndisang JF, Lane N and Jadhav A (2009) The heme oxygenase system abates hyperglycemia in Zucker diabetic fatty rats by potentiating insulin-sensitizing pathways. *Endocrinology* **150**:2098-2108.

Ndisang JF, Lane N, Syed N and Jadhav A (2010) Up-regulating the heme oxygenase system with hemin improves insulin sensitivity and glucose metabolism in adult spontaneously hypertensive rats. *Endocrinology* **151**:549-560.

Permana PA, Menge C and Reaven PD (2006) Macrophage-secreted factors induce adipocyte inflammation and insulin resistance. *Biochem Biophys Res Commun* **341**:507-514.

Pingitore A, Aquaro GD, Lorenzoni V, Gallotta M, De Marchi D, Molinaro S, Cospite V, Passino C, Emdin M, Lombardi M, Lionetti V and L'Abbate A (2011) Influence of preload and afterload on stroke volume response to low-dose dobutamine stress in patients with non-ischemic heart failure: A cardiac MR study. *Int J Cardiol*.

Poornima IG, Parikh P and Shannon RP (2006) Diabetic cardiomyopathy: the search for a unifying hypothesis. *Circ Res* **98**:596-605.

Ram R, Mickelsen DM, Theodoropoulos C and Blaxall BC (2011) New approaches in small animal echocardiography: imaging the sounds of silence. *Am J Physiol Heart Circ Physiol* **301**:H1765-1780.

Rodriguez F, Langer F, Harrington KB, Cheng A, Daughters GT, Criscione JC, Ingels NB and Miller DC (2005) Alterations in transmural strains adjacent to ischemic myocardium during acute midcircumflex occlusion. *The Journal of thoracic and cardiovascular surgery* **129**:791-803.

Rosito GA, Massaro JM, Hoffmann U, Ruberg FL, Mahabadi AA, Vasan RS, O'Donnell CJ and Fox CS (2008) Pericardial fat, visceral abdominal fat, cardiovascular disease risk factors, and vascular calcification in a community-based sample: the Framingham Heart Study. *Circulation* **117**:605-613.

Sabio G, Das M, Mora A, Zhang Z, Jun JY, Ko HJ, Barrett T, Kim JK and Davis RJ (2008) A stress signaling pathway in adipose tissue regulates hepatic insulin resistance. *Science* **322**:1539-1543.

Sammut IA, Foresti R, Clark JE, Exon DJ, Vesely MJ, Sarathchandra P, Green CJ and Motterlini R (1998) Carbon monoxide is a major contributor to the regulation of vascular tone in aortas expressing high levels of haeme oxygenase-1. *Br J Pharmacol* **125**:1437-1444.

Scazzocchio B, Vari R, D'Archivio M, Santangelo C, Filesi C, Giovannini C and Masella R (2009) Oxidized LDL impair adipocyte response to insulin by activating serine/threonine kinases. *J Lipid Res* **50**:832-845.

Senanayake GV, Banigesh A, Wu L, Lee P and Juurlink BH (2012) The dietary phase 2 protein inducer sulforaphane can normalize the kidney epigenome and improve blood pressure in hypertensive rats. *Am J Hypertens* **25**:229-235.

Tilg H and Moschen AR (2008) Inflammatory mechanisms in the regulation of insulin resistance. *Mol Med* **14**:222-231.

Tuncman G, Hirosumi J, Solinas G, Chang L, Karin M and Hotamisligil GS (2006) Functional in vivo interactions between JNK1 and JNK2 isoforms in obesity and insulin resistance. *Proc Natl Acad Sci U S A* **103**:10741-10746.

Uysal KT, Wiesbrock SM, Marino MW and Hotamisligil GS (1997) Protection from obesity-induced insulin resistance in mice lacking TNF-alpha function. *Nature* **389**:610-614.

van den Brom CE, Bosmans JW, Vlasblom R, Handoko LM, Huisman MC, Lubberink M, Molthoff CF, Lammertsma AA, Ouwens MD, Diamant M and Boer C (2010) Diabetic cardiomyopathy in Zucker diabetic fatty rats: the forgotten right ventricle. *Cardiovascular diabetology* **9**:25.

Weis N, Weigert A, von Knethen A and Brune B (2009) Heme oxygenase-1 contributes to an alternative macrophage activation profile induced by apoptotic cell supernatants. *Mol Biol Cell* **20**:1280-1288.

Yura T, Fukunaga M, Khan R, Nassar GN, Badr KF and Montero A (1999) Free-radical-generated F2-isoprostane stimulates cell proliferation and endothelin-1 expression on endothelial cells. *Kidney Int* **56**:471-478.

Zhang X, Lam KS, Ye H, Chung SK, Zhou M, Wang Y and Xu A (2010) Adipose tissue-specific inhibition of hypoxia-inducible factor 1{alpha} induces obesity and glucose intolerance by impeding energy expenditure in mice. *J Biol Chem* **285**:32869-32877.

FOOTNOTES

This work was supported by the Heart & Stroke Foundation of Saskatchewan of Canada to Dr. Joseph Fomusi Ndisang.

Disclosure statement: The authors have nothing to disclose

[†]Equal contributors

JPET Fast Forward. Published on February 26, 2013 as DOI: 10.1124/jpet.112.200808
This article has not been copyedited and formatted. The final version may differ from this version.

LEGENDS FOR FIGURES

Figure 1: Effects of the HO inducer, hemin and the HO inhibitor, SnMP, on left-ventricular HO-1, HO activity, 8-isoprostane and ET-1 of ZDF and ZL rats. (**A**) The basal HO-1 levels in ZDF rats were lower as compared to ZL-control rats. Hemin therapy increased HO-1 concentration, while the HO blocker, SnMP annulled the hemin effect. Hemin also enhanced HO activity in ZL rats, but less intensely as compared to ZDF rats. (**B**) The basal HO activity in ZDF rats was depressed as compared to ZL-control rats, but was enhanced by hemin while the HO blocker, SnMP annulled the hemin effect. Hemin also enhanced HO activity in ZL rats, but less intensely as compared to ZDF rats. Hemin reduced (**C**) 8-isoprostane and (**D**) abated ET-1 in ZDF and ZL-control rats, but SnMP abolished the effect. The vehicle dissolving hemin and SnMP had no effect on HO activity, 8-isoprostane and ET-1. Bars represent means ± SE; *n=6* rats per group (*p<0.05, **p<0.01 vs. all groups; †p<0.05, †† p<0.01 vs. Control-ZL rats).

Figure 2: The effects of hemin and the HO inhibitor, SnMP, on left-ventricular inflammatory cytokines. Hemin therapy reduced (**A**) TNF-α, (**B**) IL-6 and (**C**) IL-1β, in ZDF rats and ZL-controls, while SnMP nullified the effects of hemin. Bars represent means ± SE; *n=6* rats per group (*p<0.05, **p<0.01 vs. all groups; †p<0.01 vs. Control-ZL rats).

Figure 3: The effects of hemin and the HO inhibitor, SnMP, on left-ventricular NF-κB, AP-1 and JNK. Quantitative real-time RT-PCR indicated hemin therapy suppressed the elevated basal mRNA expression of (**A**) NF-κB, (**B**) AP-1 and (**C**) JNK in ZDF and ZL rats, but SnMP annulled the hemin effect. Bars represent means ± SE; *n*=6 rats per group (*p<0.05, **p<0.01 vs. all groups; †p<0.01 vs. Control-ZL rats).

Figure 4: Effect of hemin on left-ventricular ED-1, ED-2, IRS-1, PI3K and PKB in ZDF rats. Representative Western immunoblots and relative densitometry indicates that hemin therapy (**A**) suppressed ED-1, but enhanced (**B**) ED-2, (**C**) IRS-1, (**D**) PI3K and (**E**) PKB in ZDF. Bars represent means ± SE; *n=4* rats per group (*p<0.05 vs. control-ZDF).

Figure 5: Effect of hemin on longitudinal muscle fiber thickness is ZDF. (**A**) Representative images of histological sections revealed that hemin therapy attenuated longitudinal muscle fiber thickness is in ZDF. In untreated ZDF rats, enlarged cardiomyocytes with increscent nuclei were evident as compared to normal cardiomyocytes in age/sex-matched the ZL-control rats. (**B**) Semi-quantitative analyses revealed that hemin therapy markedly reduced longitudinal muscle fiber thickness is ZDF rats. Bars represent means ± SE; *n=4* rats per group (*p<0.05 vs. control-ZDF and control-ZL; **p<0.01 vs. control-ZL).

Figure 6: Schematic representation of the actions of hemin. Hemin therapy enhances HO-1, which in turn reduces adiposity and pro-inflammatory cytokines including IL6, IL-1β, NF-κB, TNF-α, JNK and M1-phenotype macrophage infiltration. Correspondingly, insulin sensitivity increases and normoglycemia is restored.

JPET Fast Forward. Published on February 26, 2013 as DOI: 10.1124/jpet.112.200808
This article has not been copyedited and formatted. The final version may differ from this version.

Table-1: Effect of hemin and stannous mesoporphyrin (SnMP) on physiological variables in ZDF and ZL

Physiological variables	Animal groups				
	Control ZL	ZL+ Hemin	Control ZDF	ZDF + Hemin	ZDF + Hemin +SnMP
Body weight (g)	363.7 ± 5.4	354.5 ± 9.5	383.6 ± 5.4	363.4 ± 6.5†	352.5 ± 8.2$^{\#}$
Fasting glucose (mmo/L)	7.2 ± 0.5	6.4 ± 0.3*	24.6 ± 3.1	6.8 ± 1.3**	19.2 ± 2.8$^{\#}$
Cardiac hypertrophy (g/Kg body weight)	2.7± 0.2	2.3 ± 0.1*	3.8 ± 0.3	2.4 ± 0.14**	3.4 ± 0.3$^{\#}$
Pericardial adiposity (g/Kg body weight)	1.3 ± 0.1	0.97 ± 0.05*	1.85 ± 0.2	0.79 ± 0.13**	1.72 ± 0.5$^{\#}$

$^{\dagger}p<0.05$ vs controls; $^{*}p<0.05$ vs Control ZDF or control ZL, $^{\#}p<0.05$ vs ZDF+Hemin, n=8 per group

JPET Fast Forward. Published on February 26, 2013 as DOI: 10.1124/jpet.112.200808
This article has not been copyedited and formatted. The final version may differ from this version.

Table-2: Echocardiographic and invasive hemodynamic measurements

	Hemodynamic Parameters					
Animals	Systolic BP (mmHg)	Cardiac output (ml/min)	Ejection Fraction (%)	LVSP (mm Hg)	$+dP/dt_{(max)}$ (mmHg/sec)	Total Peripheral Resistance (mmHg.min/ml)
Control ZDF	137.6 ± 3.7	82.06 ± 9.36	62.35 ± 0.93	135.05 ± 7.31	2828.74 ± 194.41	1.32 ± 0.14
ZDF+Hemin	118.4 ± 2.5*	88.76 ± 4.67	65.70 ± 1.21	131.97 ± 2.66	2575.86 ± 103.35	1.16 ± 0.08*
% improvement in ZDF+Hemin	-13.95[1]	8.26	5.37	-2.28[1]	-8.94[1]	-12.16[1]

[1]The negative percentage changes in left-ventricular systolic pressure (LVSP) and left-ventricular pressure development (+dP/dt) are well correlated to the reduction of total peripheral resistance and systolic blood pressure, all of which are indicative of improved cardiac function (Boron and Boulpaep, 2009). (*$^{*}p<0.05$ vs Control ZDF, n=6-8 per group).*

Figure 1

JPET Fast Forward. Published on February 26, 2013 as DOI: 10.1124/jpet.112.200808
This article has not been copyedited and formatted. The final version may differ from this version.

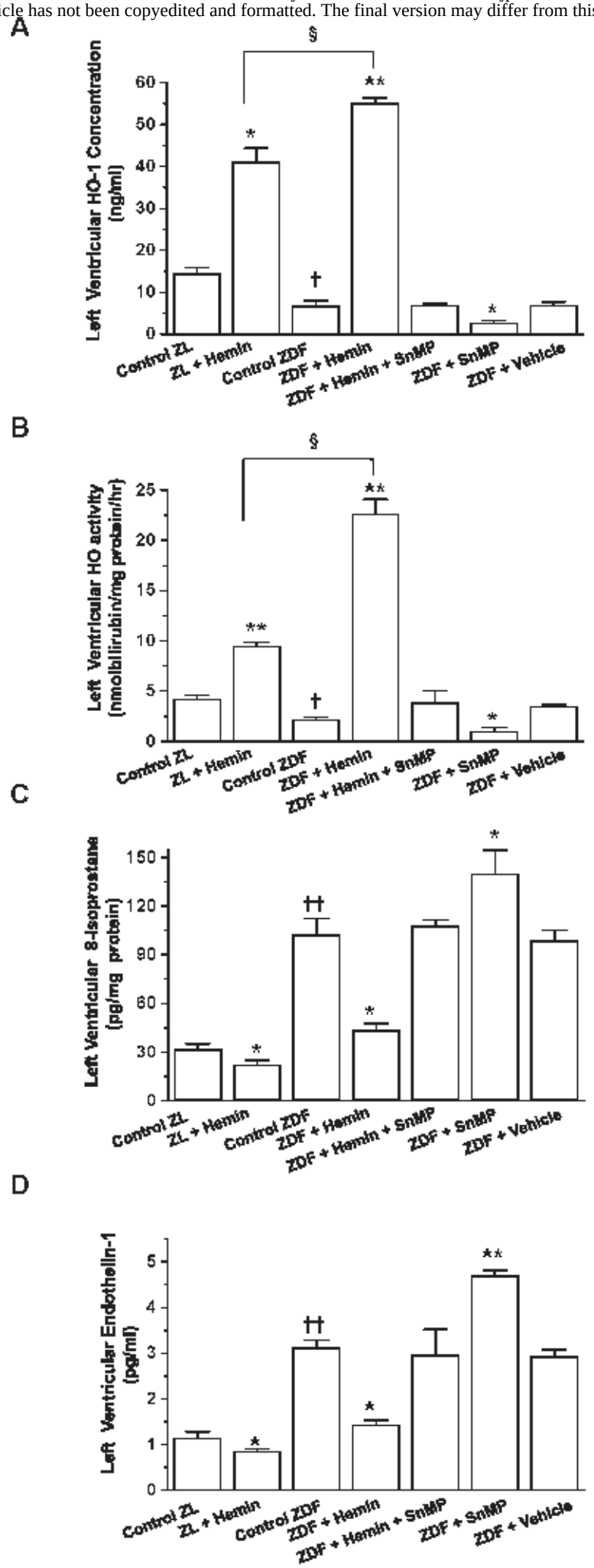

Figure 2

JPET Fast Forward. Published on February 26, 2013 as DOI: 10.1124/jpet.112.200808
This article has not been copyedited and formatted. The final version may differ from this version.

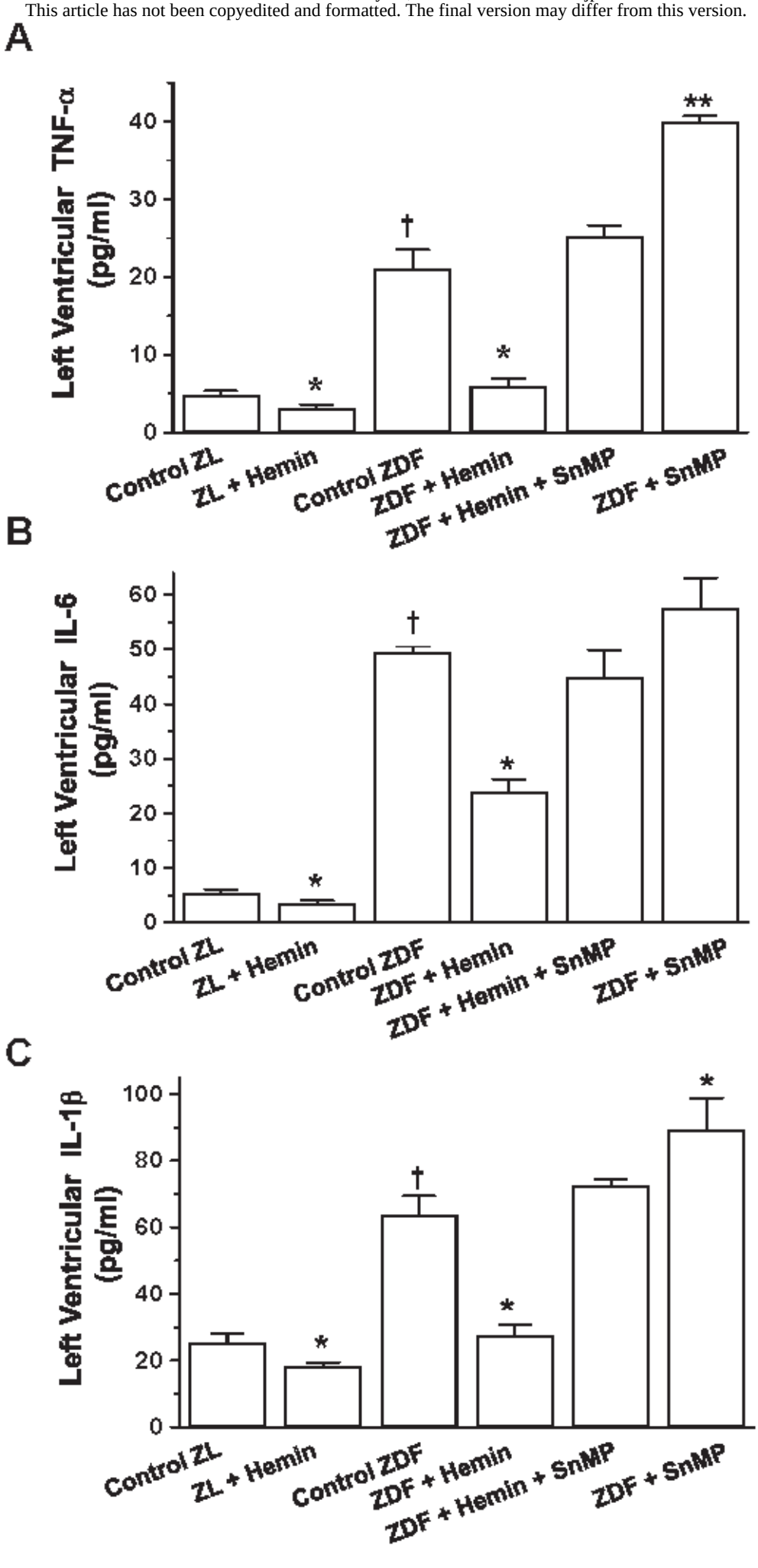

Figure 3

JPET Fast Forward. Published on February 26, 2013 as DOI: 10.1124/jpet.112.200808
This article has not been copyedited and formatted. The final version may differ from this version.

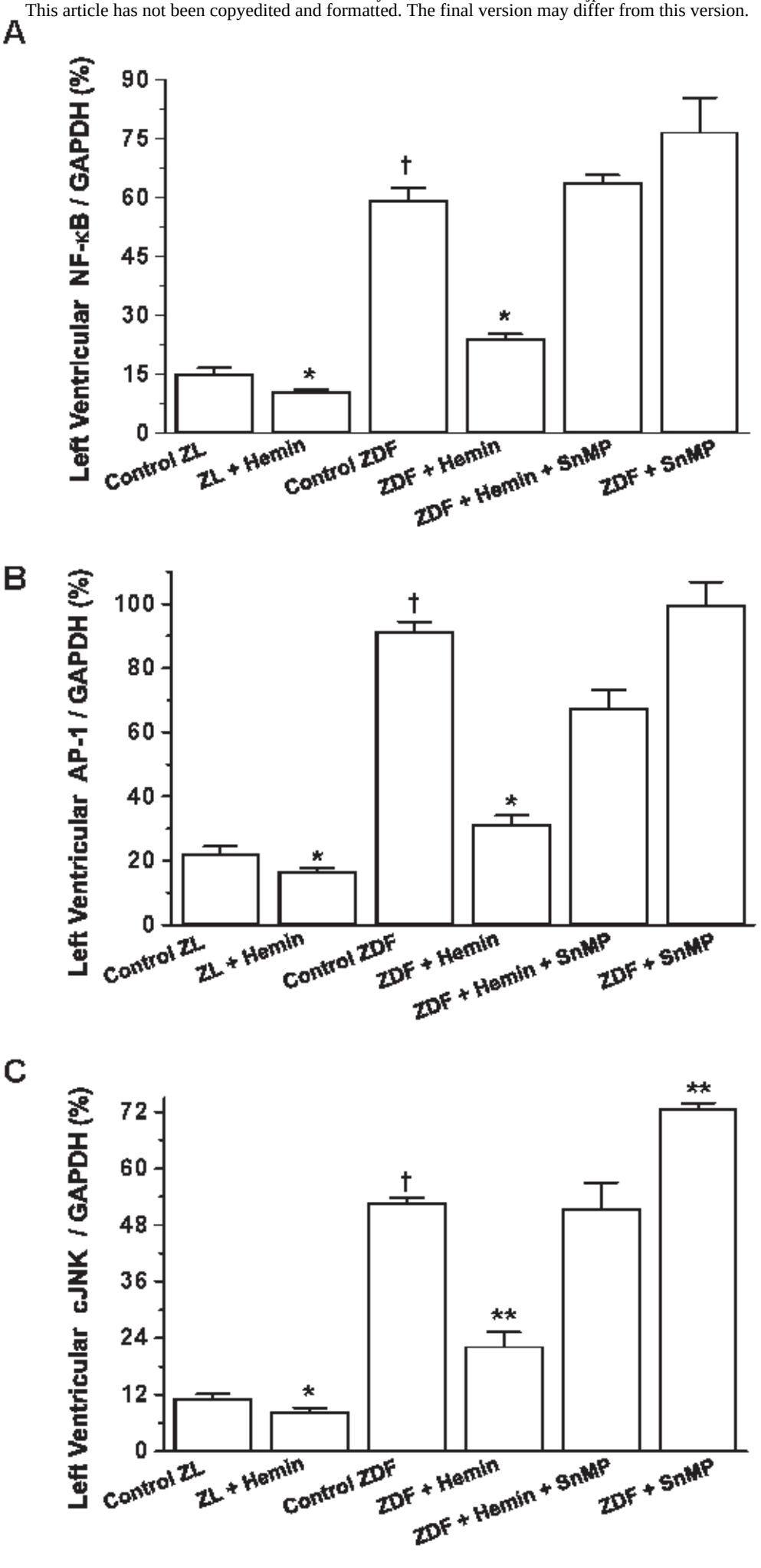

Figure 4

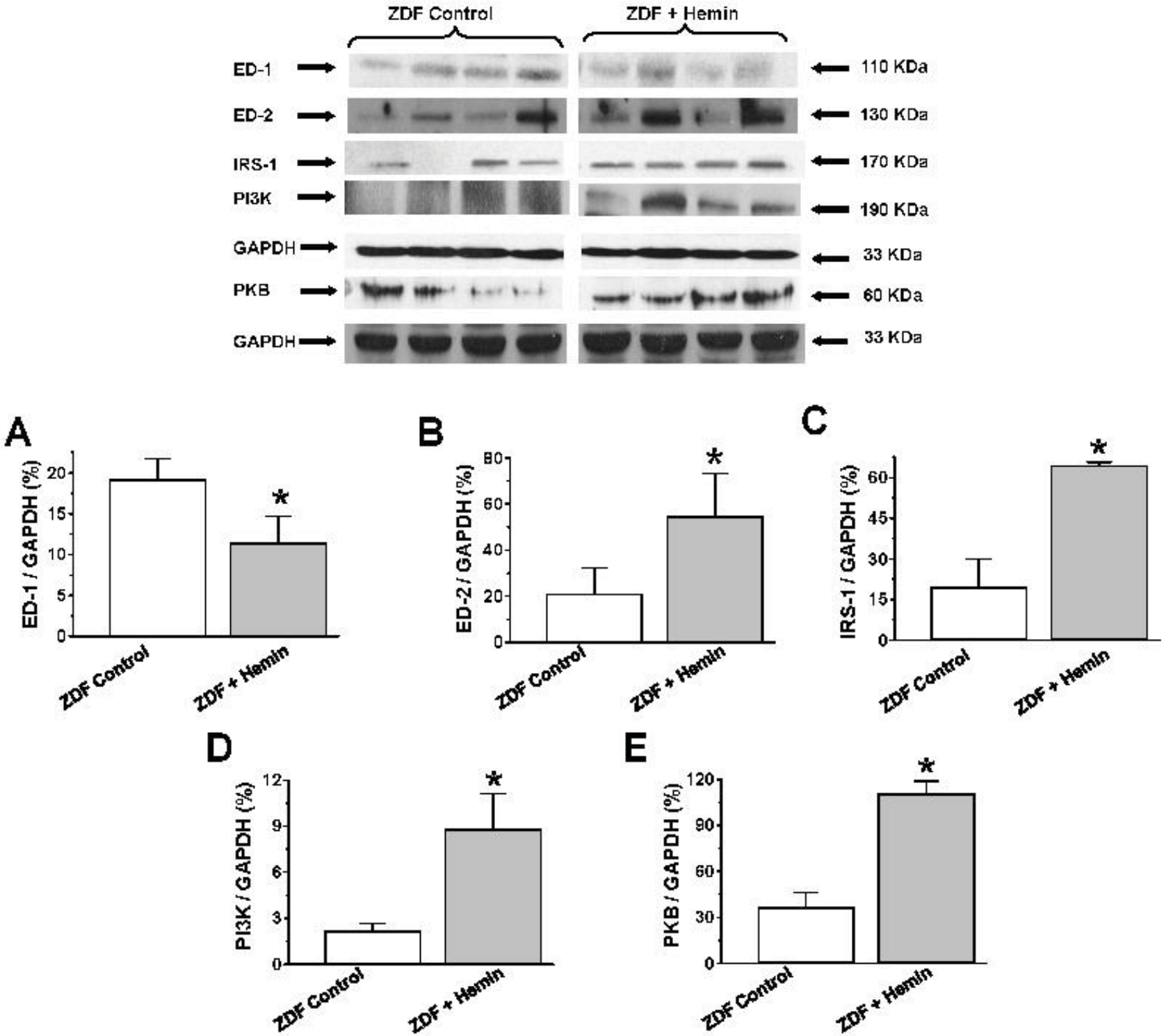

Figure 5

JPET Fast Forward. Published on February 26, 2013 as DOI: 10.1124/jpet.112.200808
This article has not been copyedited and formatted. The final version may differ from this version.

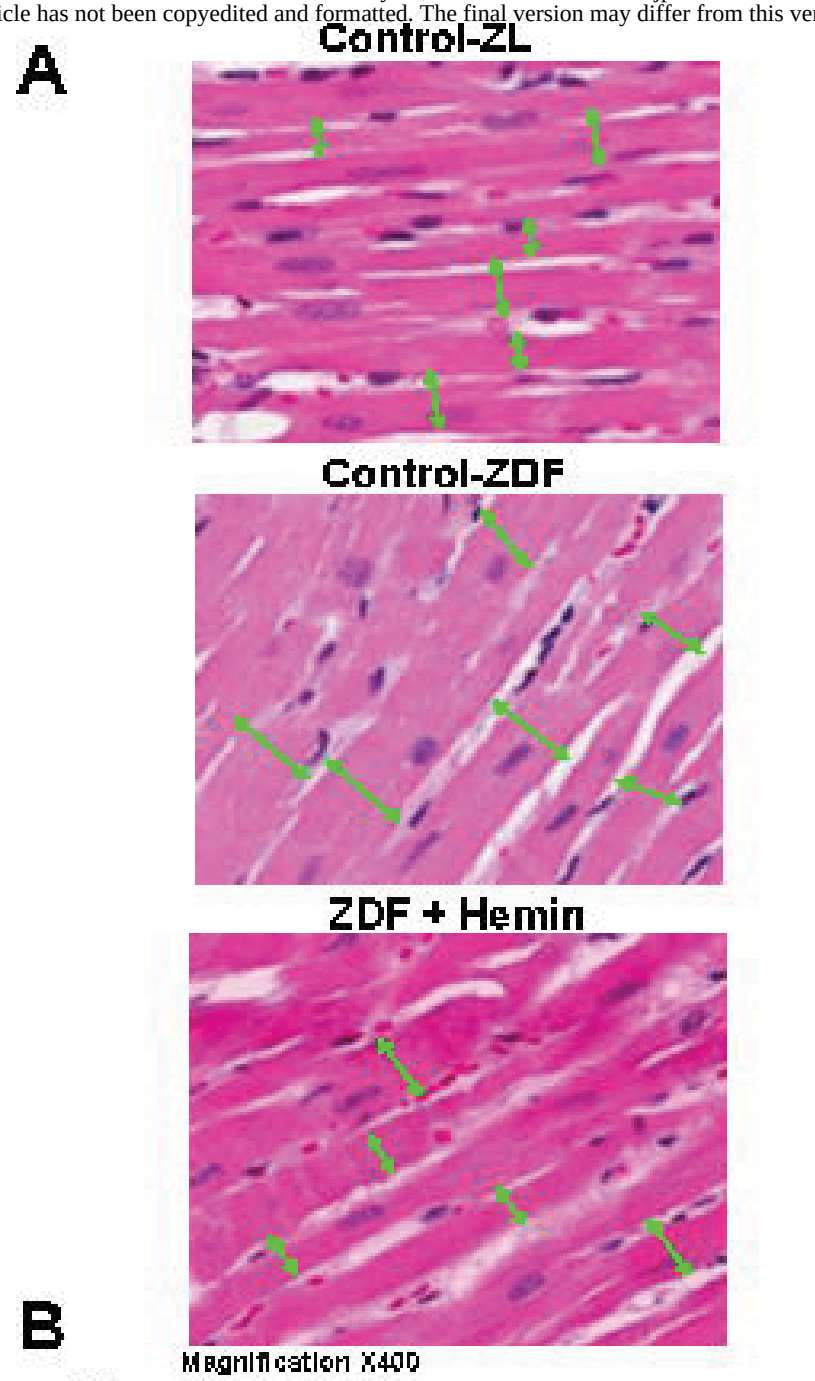

Figure 6